JMEPEG (2011) 20:102–107
DOI: 10.1007/s11665-010-9643-z
©ASM International
1059-9495/$19.00

Role of the Austenite-Ferrite Transformation Start Temperature on the High-Temperature Ductility of Electrical Steels

F. Equihua-Guillén and A. Salinas-Rodríguez

(Submitted October 13, 2009; in revised form March 3, 2010)

The austenite to ferrite transformation start temperature was measured in two low-C, Si-Al grain non-oriented electrical steels using in situ x-ray diffraction and the direct comparison method with the $(111)^{\gamma}$ and $(110)^{\alpha}$ diffracted intensities. It was shown that increasing Al content from 0.2 to 0.6 wt.% in a 0.06 wt.% C, 0.6 wt.% Si and 0.5 wt.% Mn steel increases the Ae_3 temperature from 928 to 955 °C. The results are supported by microstructural observations of isothermally transformed samples and used to discuss the loss of ductility during high temperature deformation (e.g. hot rolling) of this type of materials.

Keywords Ae_3-Ar_3 temperatures, ferrite film, GNO electrical steel, grain boundary, in situ x-ray diffraction, intergranular fracture

1. Introduction

Plain C-Mn, C-Mn-Al and microalloyed steels exhibit a complex high temperature tensile ductility behavior when plastic deformation is performed near the austenite to ferrite (Ar_3) transformation temperature under cooling conditions (Ref 1). In general, curves of reduction of area at fracture as a function of temperature exhibit a ductility "trough" which is invariably associated with intergranular fracture. Two distinct grain boundary cracking mechanisms have been suggested. Strain concentration at strain-induced ferrite films (5-20 μm thick) formed at austenite grain boundaries (Ref 2-5) causes nucleation and growth of microvoids at grain boundary inclusions and precipitates. This process leads to intergranular cracking by microvoid coalescence and the fracture surfaces are usually covered with fine ductile dimples. This mechanism takes place at temperatures between Ae_3 (the equilibrium austenite to ferrite transformation temperature) and Ar_3, where the thickness of strain-induced ferrite films does not change significantly with temperature. When deformation is performed at $T < Ar_3$, ferrite can be formed prior to deformation and, as the volume fraction increases, the ductility of the steel is recovered.

A similar mechanism has been proposed for Nb- and Al-containing steels. In this case, fine precipitation of Nb(C,N) and AlN in the austenite grains during cooling leads to formation of relatively softer precipitate-free zones (PFZ, ~500 nm thick) on both sides of the austenite grain boundaries. As a result, strain concentration at PFZ's results in nucleation and growth of microvoids at precipitate particles and coalescence leads finally to intergranular cracking at PFZ's (Ref 1). Grain boundary sliding followed by cracking can also take place in austenite due to limited dynamic recovery. Flow stresses and strain hardening rates in austenite are high and prevent relief of stress concentrations at grain boundary triple-points and particles. Thus, nucleation of grain boundary cracks leads to intergranular failure in the austenite. However, in this case, the fracture surfaces appear smooth under the SEM and ductile dimples are not observed.

The relationship between ductility and deformation temperature in grain non-oriented (GNO) electrical steels is less well known. In a prior publication (Ref 6), it was reported that, in a GNO-electrical steel containing 0.06 wt.% C, 0.6 wt.% Mn, 0.5 wt.% Si and 0.3 wt.% Al, a severe ductility loss is observed at temperatures between 950 and 1050 °C (Fig. 1). SEM analysis of fracture surfaces of specimens which exhibited low ductility showed clear evidence of intergranular cracking by a mechanism involving coalescence of microcavities formed by nucleation and growth at AlN and Si-containing second phase particles present at grain boundaries (Ref 6, 7). As can be seen in Fig. 1, the tensile ductility is recovered when the deformation temperature is increased above a 1050 °C or decreased below 900 °C. From the observed temperature dependence of the maximum flow stress observed in the experimental flow curves, García et al. (Ref 6) estimated that the Ae_3 temperature for the transformation of deformed austenite to ferrite in their steel was approximately 950 °C. It is noteworthy that the estimated Ae_3 temperature is well below the minimum temperature in the ductility trough. Furthermore, no evidence of formation of ferrite films at austenite grain boundaries was presented. Nevertheless, Garcia et al. (Ref 6) suggested that formation of strain-induced ferrite films also played a major role in the loss of ductility during high temperature deformation of GNO-electrical steel.

The Ae_3 temperature represents the maximum temperature at which strain-induced ferrite can be expected to form from

F. Equihua-Guillén and **A. Salinas-Rodríguez**, Centro de Investigación y de Estudios Avanzados del Instituto Politécnico Nacional, Unidad Saltillo, Carretera Saltillo-Monterrey Km. 13. Molinos de Rey, C.P. 25900, P.O. Box 663, Saltillo Coah, Mexico. Contact e-mails: fabianequihua@gmail.com and armando.salinas@cinvestav.edu.mx.

deformed austenite under cooling conditions. The Ar_3 and Ae_3 temperatures for the GNO-electrical steel used in the experimental study reported in Ref. [6] was estimated between 845 and 941 °C using Andrews empirical expression (Ref 8), published binary Fe-Si phase diagrams (Ref 9) and other empirical expressions reported elsewhere (Ref 10-19). All these calculated temperatures are well below the temperature at which the ductility minimum is observed in Fig. 1 (1000 °C). Thus, formation of strain-induced ferrite films cannot explain the loss of ductility observed in electrical steels alloyed with about 1 wt.% (Si + Al). It is possible, however, that the austenite to ferrite transformation temperatures (Ae_3 and Ar_3) are underestimated by the empirical equations used in the calculation. This is surely true for the case of Ar_3 (845 °C) since the expression was developed considering plain C-Mn and Nb microalloyed steels.

Because of the important role that this type of ductility loss plays during hot rolling of GNO-electrical steels, it was decided to carry out an experimental study to determine the actual Ae_3 temperature for the transformation of austenite to ferrite using an in situ x-ray diffraction technique.

Aluminum traditionally has been used almost exclusively as a grain refining or deoxidizing element in steel in amounts rarely exceeding 0.01 to 0.07 wt.%. However, Al additions can be used as a specific alloying element to improve strength by solid solution strengthening and modify toughness by processes such as solid solution softening (Ref 20). There is also great commercial interest in Al additions, of the order of 1-2 wt.%, to high strength low carbon strip steels to produce a highly desirable dual phase microstructure containing retained austenite for cold forming applications. A recent review on dual-phase and transformation induced plasticity (TRIP) steels (Ref 21) concluded that there is much to learn about the role of Al on transformation behavior of these types of steel. In Si-Al containing electrical steels, Al plays a similar role as Si in increasing the resistivity and, therefore, reducing core losses in electrical motors.

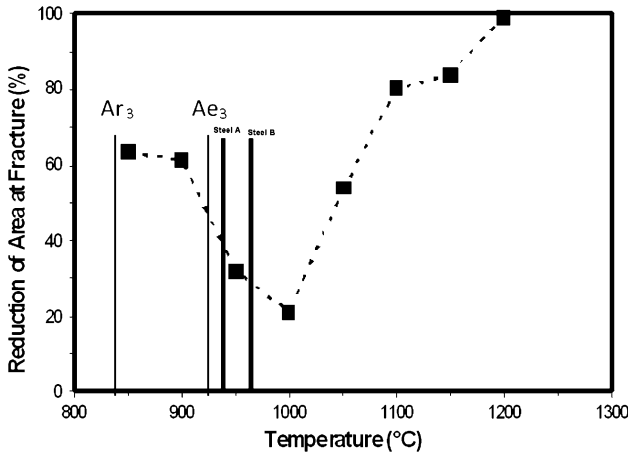

Fig. 1 Effect of deformation temperature on the tensile ductility of low C, Si-Al GNO-electrical steels austenitized at 1250 °C for 15 min and deformed at 5×10^{-4} s^{-1} (Ref 6). The *thin vertical lines* are at the positions of the Ae_3 and Ar_3 temperatures calculated from the chemical composition of the steel (Ref 6, 8, 9). The *thick vertical lines* are at the positions of the Ae_3 temperatures measured by in situ x-ray diffraction for steels A and B in this work

2. Experimental Procedure

Two 3.5 mm thick hot rolled GNO-electrical steel strips were obtained from a local supplier. Chemical analysis was performed by optical emission spectrometry and the LECO combustion technique for C and S. The chemical compositions of the strips are listed in Table 1.

Samples, 9 mm wide and 15 mm long, were cut from the strips and machined to a thickness of 0.8 mm. After that, the samples were ground on progressively finer SiC abrasive papers up to a final thickness of 0.3 mm. Finally, the samples were polished using 0.3 μm diamond paste. The effect of temperature on the x-ray diffractions of these samples was determined using an Anton-Paar high temperature chamber adapted to a multipurpose Philips x-ray diffractometer. This system uses a Pt-filament (1 mm thick, 9 mm wide, 132 mm long) both as heating element and specimen holder. Protection of the Pt-filament and the sample against oxidation was provided by a continuous flow of high purity He gas in the chamber. Measurement and control of the temperature during the experiments were performed within 2 °C using a Pt/Pt-10%Rh thermocouple spot welded to the back of the Pt-filament.

The specimens were heated at a rate of 1 °C/s up to 1050 °C and soaked for 5 min. After that, the samples were first continuously cooled to 1000 °C at a rate of 1 °C/s and then in a stepwise manner at the same rate with a step size of 10 °C. X-ray diffraction patterns from 42 to 45° 2θ (300 s measurement time) were recorded at every temperature step from 1000 to 720 °C. Within this angular range, the $(110)^{\alpha}$ and $(111)^{\gamma}$ diffraction peaks of the ferrite and austenite phases appear at about 44.6 and 43.2° 2θ, respectively. The austenite-ferrite transformation temperatures were estimated from the effect of temperature on the intensity of the recorded diffraction peaks.

In order to follow the changes in microstructure produced by the transformation on cooling, a set of samples prepared from steel B were subjected to isothermal transformation treatments with holding times similar to those applied during the "in situ" x-ray diffraction experiments. In order to monitor the temperature of the specimens a K-type thermocouple was spot welded at the end of each specimen that had the same dimensions as the specimens for x-ray diffraction. In this case, the samples were heated to 1050 °C at a rate 7 °C/s and soaked during 5 min in a muffle furnace. After that, a stepwise cooling ramp of 0.15 °C/s with holding periods of 300 s every 10 °C was set in the furnace. After each temperature step a sample was extracted

Table 1 Chemical composition of A and B GNO electrical steels (wt.%)

Steel	C	Al	Si	Mn	Mo	S	P	Cu	Cr	V	Ni	Ti
A	0.06	0.22	0.61	0.5	0.0092	0.0005	0.001	0.11	0.017	0.0004	0.046	0.001
B	0.06	0.61	0.61	0.5	0.0095	0.0005	0.001	0.12	0.016	0.00192	0.054	0.002

and quenched into a brine bath at 5 °C. Finally, the quenched samples were prepared for metallographic examination using a reflected light microscope.

3. Results and Discussion

3.1 Effect of Temperature on the Austenite to Ferrite Transformation Temperature

Figures 2a and b show the effect of temperature on the x-ray diffraction patterns measured every 10 °C from 1000 to 720 °C. As can be seen, the $(110)^{\alpha}$ and $(111)^{\gamma}$ peaks appear at about 44.6 and 43.4°, respectively. The patterns show changes in the intensities of these peaks as a function of temperature. It can be appreciated that austenite is the only equilibrium phase at 1000 °C. As can be seen in Fig. 2a, for the case of specimen A, the ferrite phase appears first at ~930 °C and the austenite-ferrite transformation ends at ~855 °C. In contrast, in the case of specimen B with a higher Al content, the ferrite phase appears first at ~955 °C and ends at ~890 °C.

The results of these measurements indicate that, in the present GNO-electrical steels, increasing the Al content causes an increase of about 23 °C in the temperature at which austenite starts to decompose into ferrite and a decrease of about 10 °C in the temperature range where austenite and ferrite coexist.

3.2 Effect of Al Content on the Austenite to Ferrite Transformation Temperature

The experimental results, described in the previous section, show that increasing the aluminum content in the present electrical steel increases the austenite to ferrite transformation start temperature and decreases the temperature range where austenite and ferrite coexist. Figure 3 shows the results of a calculation using Thermo-Calc Software of the effect of C and Al content on the phase boundaries for Fe-C-Si-Al alloys. The calculations were carried out keeping Si and Mn contents constant (0.6, 0.5 wt.%, respectively). The solid and dashed lines in Fig. 3 give the effect of C on the austenite-ferrite equilibrium temperatures (Ae_3) for electrical steels A and B, respectively. As can be seen, for alloys with 0.06 wt.% C, 0.6 wt.% Si and 0.5 wt.% Mn, increasing the Al content from 0.22 to 0.61 wt.% causes an increase in the Ae_3 temperature from 912.5 to 962.5 °C. These temperatures are close to those determined experimentally by the in situ x-ray diffraction technique used in the present work and confirm that Al and Si have a synergistic effect on the austenite to ferrite transformation temperature in this type of steels. The synergistic effect of Si and Al was corroborated using Thermo-Calc software; increasing Al content, increases Ae_3. Al has not a strong effect on transformation temperatures as the Si, however, Al has an additive effect to the Si; both alloying elements considerably increase the transformation temperatures.

3.3 Formation of Ferrite at Austenite Grain Boundaries

Figure 4 illustrates the effect of quenching temperature on the room temperature microstructure of samples of steel B

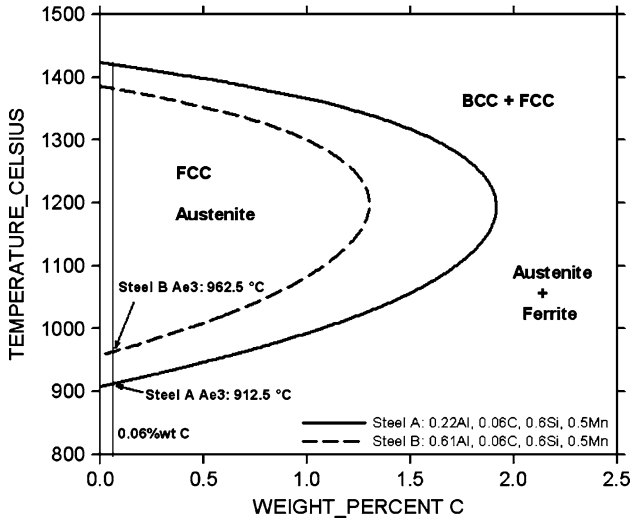

Fig. 3 Thermo-calc simulation of Fe-Si-C-Al diagram for chemical composition of specimens A and B

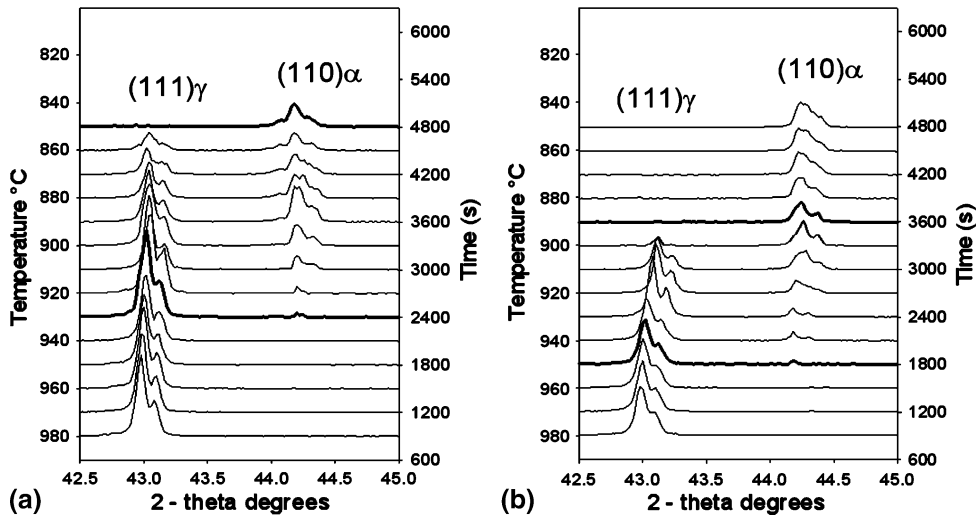

Fig. 2 Effect of temperature on the x-ray diffraction patterns of low C, Si-Al electrical steel during cooling. (a) Steel A and (b) steel B

(0.6 wt.% Al) isothermally treated during 300 s at 997, 965, 900, 850 and 790 °C. The M_s martensite start temperature calculated from the chemical composition of this steel was 495 °C. As can be seen, the microstructures of samples quenched from 965 and 997 °C are practically 100% martensite, although a very small amount of allotriomorphic ferrite is observed at prior austenite grain boundaries. These microstructures indicate that the samples were fully austenitic at the moment of quenching, i.e. $T > Ae_3$. The formation of very small amount of allotriomorphic ferrite above 950 °C is mainly due to low cooling rate during quenching. On the other hand, XRD may not be sensitive enough to detect very small amount of ferrite (<5%), both situations show a minor discrepancy between the XRD and the optical micrograph data.

In contrast, samples quenched from 950, 900 and 850 °C exhibit microstructures consisting of increasingly larger amounts of grain boundary allotriomorphic ferrite and martensite. According to Zener (Ref 22) allotriomorphic ferrite nucleates at austenite grain boundaries and grows isothermally following a parabolic time law. In the present experiments the isothermal transformation time was held constant (300 s) and the transformation temperature was decreased. As shown in Fig. 4, decreasing the transformation temperature causes coarsening of the ferrite allotriomorphs and, therefore, the microstructural evidence suggests that the transformation rate constant increases as the temperature decreases within the austenite + ferrite phase field for Si-Al electrical steels.

When the transformation temperature is decreased below the temperature at which the austenite peak was no longer observed in the diffraction pattern, the morphology of the ferrite phase changes to equiaxed and the martensite is no longer observed. This change in microstructure can be better appreciated in the SEM micrographs of Fig. 5. As can be seen, the martensite formed in the sample quenched from 965 °C appears as sets of very thin parallel laths which are either parallel or perpendicular to the prior austenite grain boundaries. In contrast, in the sample quenched from 790 °C the transformation product exhibits a coarse platelet morphology where individual platelets nucleated mostly perpendicular to the ferrite grain boundaries. Growth of these platelets ends at the center of the transformed region and some very fine particles (presumably Fe-carbides) appear to have precipitated between platelets. This type of microstructure is similar to bainite. It is noteworthy that pearlite was not found in any of the microstructures of the samples transformed at temperatures as low as 720 °C.

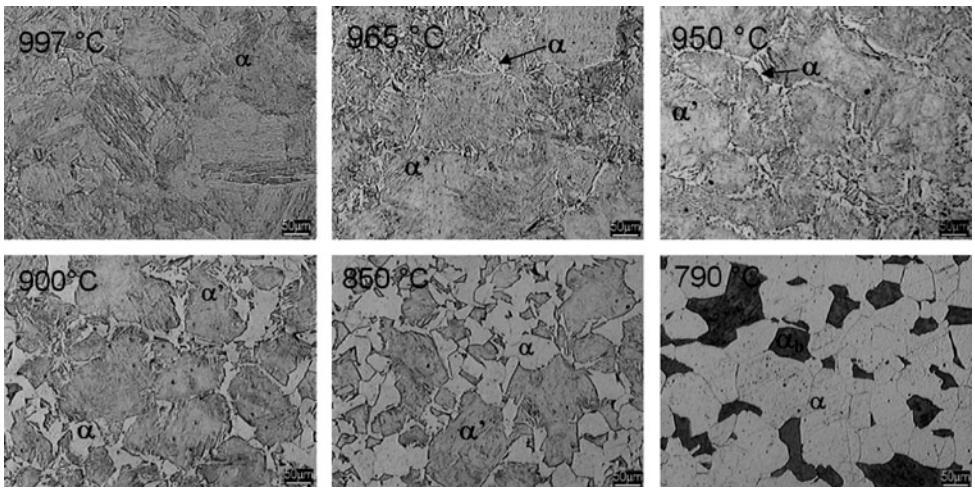

Fig. 4 Room temperature microstructures of samples of steel B cooled from 1050 °C to the indicated temperatures, held during 300 s and finally quenched

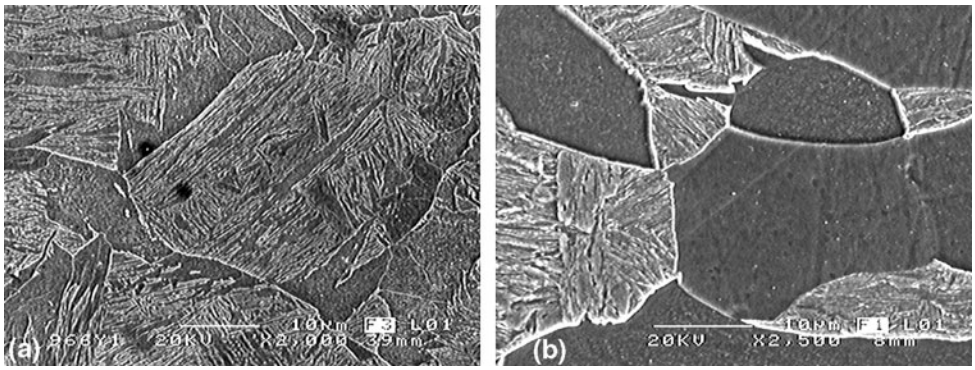

Fig. 5 Microstructures of samples of steel B cooled from 1050 °C to (a) 965 °C, (b) 790 °C, held during 300 s and finally quenched to room temperature

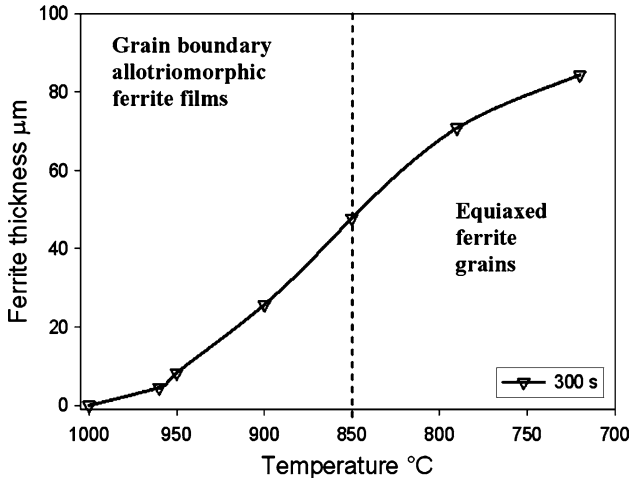

Fig. 6 Effect of temperature on the "size" of the ferrite formed isothermally at temperatures between 965 and 720 °C

Finally, Fig. 6 shows the effect of temperature on the size of the ferrite observed in the microstructures of Fig. 4. In the case of samples quenched from 965 to 850 °C, the data represents the average thickness of the grain boundary allotriomorphic ferrite while, for samples quenched from lower temperatures, the size represents the average equiaxed ferrite grain size. As can be seen, samples quenched from $Ae_3 > T > 950$ °C exhibit ferrite films of less than 10 µm in thickness. Isothermal transformation at lower temperatures causes a rapid linear increase of the ferrite thickness.

3.4 Role of Ferrite Films During High-Temperature Deformation of GNO-Electrical Steels

The Ae_3 temperatures (930 and 955 °C) determined from the x-ray diffraction data correspond to undeformed austenite. Although Ar_3 temperatures under continuous cooling conditions are lower than Ae_3 temperatures, the measured temperatures can be taken as an estimation of the maximum temperature at which strain-induced ferrite can be expected to form from deformed austenite during hot rolling. As can be seen in Fig. 1, although the measured Ae_3 are closer to the temperature of minimum ductility, formation of strain induced ferrite films cannot account for the decreased ductility observed in these steels at temperatures between the measured Ae_3 and approximately 1075 °C. In previous work, García et al. (Ref 6) studied specimens deformed at 1100 and 900 °C of electrical steels, the samples exhibited ductile fracture originated by coalescence of microcavities. The fracture surface of sample deformed at 1100 °C shows minor quantity of microcavities with respect to the sample deformed at 900 °C. Nevertheless, the sample deformed at 1100 °C shows bigger size of microcavities compared with the sample deformed at 900 °C. This latter observation suggests that, the ductility loss at $950 < T < 1050$ °C, can be attributed to the formation of thin ferrite films around the prior austenite grain boundaries during hot deformation. Thus, concentration of plastic deformation occurs in this region due to the low resistance of ferrite, causing rapid coalescence of microcavities at the austenite/ferrite interface. This process is accelerated by AlN particles formed in the grain boundaries of austenite during cooling to the deformation temperature. On the other hand, MnS particles promote nucleation sites for AlN precipitation (Ref 23, 24) during cooling in the austenite field; therefore, the quantity of these particles can be high in this kind of steel. The loss of ductility within this temperature range may be associated with some kind of weakening effect on austenite grain boundaries. The observed loss of ductility at temperatures greater than Ae_3 measured in this work needs further investigation.

Recently, Palizdar et al. (Ref 25) carried out an interesting characterization of the transformation microstructures of low nitrogen Fe-Al alloys (up to 1 wt.% Al) using a high resolution FEG-SEM. Their results showed that solute Al can affect the austenite/ferrite interface by grain boundary segregation and strongly influence the austenite to ferrite transformation temperature and transformation behavior. According with results of the present investigation, grain boundary segregation of Al could cause a local increase in the Ae_3 and result in formation of thin grain boundary ferrite films at temperatures higher than those observed in the present work. However, this speculation needs further investigation.

Hot rolling of Si-Al electrical steels (with about 1 wt.% Si + Al) is usually performed at temperatures between 1150 and 880 °C. Thus, the presence of ferrite during hot rolling is unavoidable and the results presented in this work indicate that these materials are highly susceptible to intergranular cracking during processing.

4. Conclusion

The presence of ferrite during hot rolling of Si-Al GNO-electrical steels is unavoidable. The data presented in this paper showed that both the austenite decomposition starting temperature and the range of austenite/ferrite coexistence increase with increasing the total amount Si + Al in the electrical steel. Thus, these elements have a synergistic effect on the transformation. Formation of strain induced ferrite films can only partially account for the reduced ductility observed in these steels. It is suggested that further research is needed to understand the ductility loss observed during deformation at temperatures higher than the measured Ae_3 and up to approximately 1075 °C.

Acknowledgment

The financial support from the Consejo Nacional de Ciencia y Tecnología (CONACYT) of Mexico is gratefully recognized.

References

1. B. Mintz, S. Yue, and J.J. Jonas, Hot Ductility of Steels and Its Relationship to the Problem of Transverse Cracking During Continuous Casting, *Int. Mater. Rev.*, 1991, **36**(5), p 187–217
2. G.I.S.L. Cardoso and S. Yue, *Proceedings of the AIME Mechanical Working and Steel Processing Conference*, Vol 31, 1989, p 585
3. J.Y. Fu, C.I. Garcia, S. Pytet, and A.J. DeArdo, *Proceedings of the Processing. Microstructure and Properties of HSLA Steels*, TMS-AIME, Warrendale, PA, 1988, p 27–38
4. A. Cowley, R. Abushosha, and B. Mintz, Influence of Ar3 and Ae3 Temperatures on Hot Ductility of Steels, *Mater. Sci. Technol.*, 1998, **14**, p 1145–1153

5. B. Mintz, R. Abushosha, and M. Shaker, Influence of Deformation-Induced Ferrite, Grain-Boundary Sliding, and Dynamic Recrystallization on Hot Ductility of 0.1–0.75 % C Steels, *Mater. Sci. Technol.*, 1993, **9**, p 907–914
6. E.O. García-Sánchez, E.A. Treviño-Luna, A. Salinas-Rodríguez, and L.A. Leduc-Lezama, Mecanismos de fractura a alta temperatura en aceros eléctricos no-orientados, *Rev. Metal.,* 2007, **43**(4), p 266–271
7. E.O. García Sánchez, "Mecanismos de Fragilización a Alta Temperatura de Aceros Si-Al," Ph.D. Thesis, Cinvestav Saltillo, México, 2006
8. A.P. Guliaev, Metallography, 2nd ed., Vol 1, MIR, Moscú, 1978
9. The Making Shaping and Treating of Steel. Factors Affecting Magnetic Properties, Fe-Si-C Diagram, Silicon-Steel Electrical Sheets, 9th ed., 1998, p 1117–1128, 1157–1162
10. R. Barbosa, *Conference Proceedings of the Processing, Microstructure and Properties of HSLA Steels*, A.J. DeArdo, Ed., TMS- AIME, 1988, p 51–61
11. F. Boratto, R. Barbosa, S. Yue, and J.J. Jonas, *Conference Proceedings of the THERMEC-88*, ISIJ, Tokyo, 1988, p 383–390
12. F.H. Samuel, S. Yue, J.J. Jonas, and B.A. Zbinden, Modeling Testing of Flow Stress and Rolling Load of a Hot Strip Mill by Torsion, *ISIJ Int.,* 1989, **29**(10), p 878–886
13. S. Yue and J.J. Jonas, The Three Critical Temperatures of Steel Rolling and Their Experimental Determination, *Mater. Forum*, 1990, **14**(44), p 245–252
14. J.J. Jonas, *Conf. Proc. Mathematical Modelling of Hot Rolling of Steel*, S. Yue, Ed., CIM/ICM, 1990, p 99–118
15. F.H. Samuel, S. Yue, and J.J. Jonas, *Recrystallization '90: International Conference on Recrystallization in Metallic Materials*, T. Chandra, Ed., TMS-AIME, 1990, p 325–330
16. S. Yue and J.J. Jonas, *33rd Conference Proceedings, Mechanical Working and Steel Processing*, Vol XXIX, ISSAIME, 1992, p 275–281
17. D.Q. Bai, *Proceedings of the International Conference on Processing, Microstructure and Properties of Microalloyed and Other Modern High Strength Low Alloy Steels*, A.J. DeArdo, Ed., ISS-AIME, 1992, p 165–173
18. D.Q. Bai, S. Yue, W.P. Sun, and J.J. Jonas, Effect of Deformation Parameters on the No-Recrystallization Temperature in Nb-Bearing Steels, *Met. Trans. A* 1993, **24**(A), p 2151–2159
19. I. Tamura, *Thermemechanical Processing of High Strength Low Alloy Steels*, Butterworths, 1988, p 162
20. B. Mintz, *Proceedings of the International Conference, TRIP Aided High Strength Ferrous Alloys*, B.C. DeCooman, Ed., Ghent, Belgium, 2002, p 379–382
21. M. De Meyer, B.C. DeCooman, and D. Vanderschueren, *Proceedings of the International Conference on Thermomechanical Processing of Steels*, IoM London, 2001, p 505–514
22. C. Zener, Theory of Growth of Spherical Precipitates From Solid Solutions, *J. Appl. Phys*, 1949, **20**, p 950–953
23. F.G. Wilson and T. Gladman, Aluminium Nitride in Steel, *Int. Mat. Rev*, 1988, **33**(5), p 221–286
24. K. Ushioda, O. Akisue, K. Koyama, and Y.T. Hayashida, *Developments in the Annealing of Sheet Steels*, R. Pradhan and I. Gupta, Ed., The Minerals Metals and Materials Society, 1992, p 261–286
25. Y. Palizdar, R.C. Cochrane, R. Brydson, F. Bygrave, and A.J. Scott, Understanding the Role of Aluminium in Low Level Nitrogen Steels via Microstructural Characterization, *J. Phys.* 2008, Conference Series, Vol 126, p 012–019